

Quantum correlations of two optical fields close to electromagnetically induced transparency

A. Sinatra

Laboratoire Kastler Brossel, ENS, 24 Rue Lhomond, 75231 Paris Cedex 05, France

For two cavity modes exciting a transition close to electromagnetically induced transparency we show the existence of a universal dispersive bistability curve dividing the parameter space into two regions in which the system acts either as an ideal "squeezer" or a quantum non-demolition device. We use a fully quantum 3-level model including cavity losses and spontaneous emission to calculate mean field intensities and quantum fluctuations as a function of the cavity length that could be directly compared with experiment. Simple analytical predictions are obtained in the good cavity limit in which the atomic variables are adiabatically eliminated.

PACS numbers: 42.50.Dv, 42.50.Gy, 42.65.Pc

Electromagnetically induced transparency (EIT) which has recently received a lot of attention in the context of slow light in an atomic medium [1], has played a key role in quite different contexts including sub-recoil laser cooling [2], lasing without inversion [3], nonlinear quantum optics [4] and spin squeezing [5]. Already in the early eighties, theoretical studies showed that a lambda three-level medium close to the EIT conditions can be used to obtain single mode optical bistability due to nonlinear absorption [6], and squeezing [7]. More recently intensity correlations (and anti-correlations) between two fields close to EIT were experimentally observed [8]-[9]. In this paper we consider two cavity modes interacting with an ensemble of atoms in a configuration close to EIT conditions i.e. detuned by a small amount across the respective atomic resonances (Fig. 1). To the first order in the small two-photon detuning, the atomic response is purely dispersive with the consequent advantage of keeping absorption negligible avoiding to a large extent the incoherent noise coming from spontaneous emission. For equal input intensities of the two fields we show the existence of a universal dispersive bistability curve for the intracavity intensity of the fields which divides the parameter space into two parts: for input intensities higher than the bistability threshold the quantum fluctuations of the fields become quadrature dependent and can be reduced in a quadrature, while for input intensities lower than the bistability threshold crossed phase-intensity quantum correlations build up between the two fields that can be used to perform an efficient quantum non-demolition (QND) measurement of the intensity fluctuations of one field [10]. The system becomes a perfect "squeezer" or an ideal QND device at the turning point.

For $j = 1; 2$ let $\hbar \omega_{a_j}$ be the energy of the atomic transition driven by the field j . We define $\delta_j = \frac{\omega_{a_j} - \omega_j}{\gamma_j}$ the atomic detunings normalized to the decay rate of the optical coherences $\gamma_w = (\gamma_1 + \gamma_2)/2$ where $\gamma_1 + \gamma_2$ is the total population decay rate of the upper level. $C_j = \frac{g_j^2 N}{\gamma_j}$ are the cooperativity parameters where g_j are the coupling

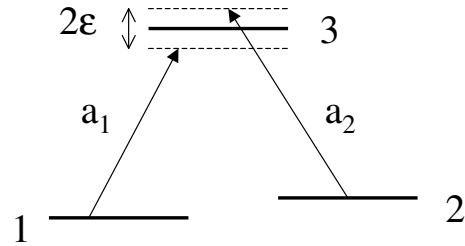


FIG. 1: Two cavity modes interact with the atoms in a configuration close to EIT conditions

constants for the two considered transitions, N is the number of atoms, γ_j are the decay rates for the two cavity fields and $\delta_j = \frac{\omega_{a_j} - \omega_j}{\gamma_j}$ are the normalized cavity detunings. We introduce normalized variables proportional to the intracavity and input fields $x_j = \frac{\sqrt{2}g_j}{\omega} \hbar a_j$ and $y_j = \frac{\sqrt{2}g_j}{\omega} \sqrt{\frac{p_j}{T_j}} E_j^{\text{in}}$ respectively, where T_j is the (input-output) mirror transmissivity for the field j . The master equation and the semiclassical equations describing the system with two cavity fields are given and discussed in detail in [11] with the same notations introduced here.

Let us consider a set of parameters symmetric for the two transitions: $\gamma_j = \gamma_j$, $C_j = C$, $\delta_j = \delta$, $\gamma_j = \gamma_j$, $\delta_j = 0$ (empty cavity resonance for both fields), and let $\gamma_1 = \gamma_2 = \gamma$ be small and positive. In Fig. 2 we show in rescaled units the stationary intensities of the intracavity fields $I_j = \langle x_j^2 \rangle = 4C$ as a function of the intensity of the input fields $Y = \langle y_j^2 \rangle = 4C$. We plot with a full line a solution with $I_1 = I_2$ displaying bistability for $Y > 1$. The negative slope branch (thin line in the figure) is unstable. The lower stable branch is very close to zero intensity and will play no role in the following. For $Y < 1$ we get two other solutions with $I_1 \neq I_2$. In the figure we show one of them with $I_1 > I_2$. The second one is obtained by exchanging I_1 and I_2 . Both solutions are stable in the considered case $\gamma_1 = \gamma_2 = 0$. We choose now two values of the input intensities, in turn above and below the bistability threshold $Y_{\text{TP}} = 1$ and we let the cav-

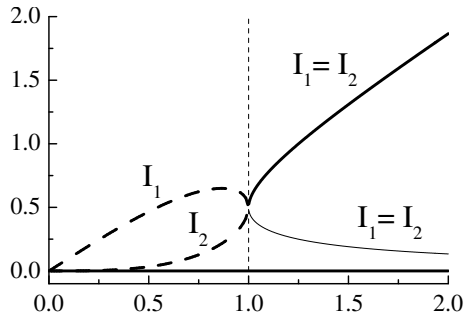


FIG. 2: Rescaled stationary intensities of the intracavity fields I_1 , and I_2 as a function of the rescaled intensity of the input fields Y . In full line the solution $I_1 = I_2$. The thick (thin) line correspond to stable (unstable) solutions. In dashed line one of the two stable solutions with $I_1 \neq I_2$. Parameters: $\gamma_1 = \gamma_2 = 0.25$ and $C_1 = C_2 = 100$, $\delta_1 = \delta_2$, $\delta_1 = \delta_2 = 0$.

ity detunings vary in Fig. 3. These kind of curves, here obtained by dynamical integration of semiclassical equations while sweeping slowly the cavity detunings forwards and backwards, can be easily achieved experimentally by sweeping the cavity length [12]–[11]. We vary δ_1 and δ_2 keeping them always equal which would imply the use of two driving fields of close optical frequencies $\omega = \omega_1$ (and for example different polarizations). For $Y = 1.1$

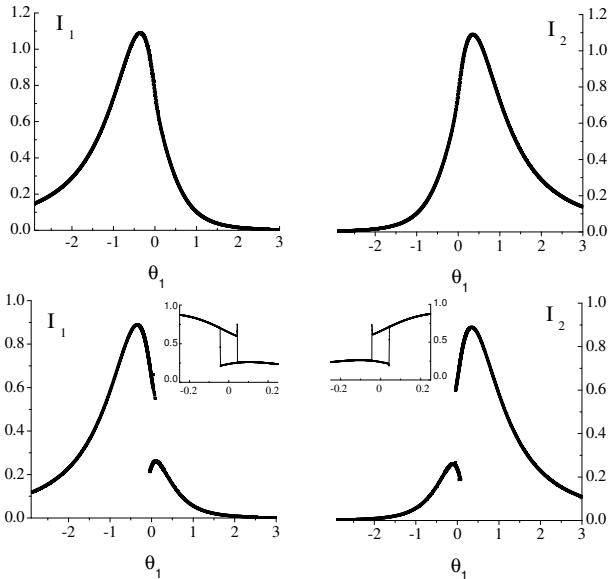


FIG. 3: Intracavity field intensities I_1 (left half), I_2 (right half) across the cavity scan. Upper half: $Y = 1.1$. Lower half: $Y = 0.9$. The other parameters are as in Fig. 3. In the inserts we point out a tiny bistability region around $\delta_1 = 0$.

ie. 10% above the bistability turning point (upper half of Fig. 3) the stable solutions for the intracavity intensities are Lorentzian-looking curves symmetrically shifted by a small amount from their empty-cavity positions for both fields. Only for $\delta_1 = \delta_2 = 0$ the two fields have the same stationary amplitude in the cavity corresponding

to the stable high-transmission branch of the bistability curve in Fig. 2. For $Y = 0.9$ i.e. 10% below Y_{TP} (lower half of Fig. 3) the situation is rather different: the stable solution for the two fields switches between a high-intensity and a low-intensity curve being always $I_1 \neq I_2$ although $\gamma_1 = \gamma_2$. In contrast with the previous case this situation is very far from the independent-fields EIT solution and the fields are in fact strongly coupled. The quantum fluctuations counterpart of Fig. 3 (top) is shown in Fig. 4 (top) where squeezing of the output fields optimized with respect to the quadrature S_j^{best} ($\delta_j = 0$) is plotted as a function of the cavity detuning. For a given quadrature of the j^{th} field $X_j = a_j e^{i\omega t} + i a_j^y e^{i\omega t}$. The squeezing spectrum is defined as

$$S_j(\omega) = 1 + 2 \int_{-\infty}^{\infty} e^{i\omega t} \langle X_j(t) X_j(0) \rangle dt \quad (1)$$

where X_j denotes the time dependent fluctuation of the operator X_j around a steady state point. The column indicates normal and time ordering for the product inside the mean. $S_j = 1$ is the shot noise and $S_j = 0$ means total suppression of fluctuations in the quadrature X_j . A large amount of squeezing is present in both fields close to $\delta_1 = 0$. Although the maximum squeezing improves getting closer (from the right) to the turning point, it is not convenient to set too near to Y_{TP} because the best squeezing curve becomes "funnel shaped" with a large dip from 1 to 0.5 and a narrow tail reaching 0 in correspondence of $\delta_1 = 0$. As one can see from Fig. 3 (top) the two fields are well transmitted by the cavity for $\delta_1 = 0$, and the system efficiently converts the input coherent beams into bright squeezed beams. The case below Y_{TP} is shown in the lower panel of the same figure where we plot across the cavity scan the coefficients C_s , C_m and $V_{s,jn}$ characterizing a QND measure of the amplitude quadrature X of one field (called the signal) performing a direct measurement on the phase quadrature Y of the other field (called the meter). The useful quantum correlations are calculated by a linearized treatment of quantum fluctuations around the stable stationary solution as in [11]. Among the three coefficients: C_s quantifies the non-destructive character of the measurement, C_m its accuracy and $V_{s,jn}$ refers to the "quantum state preparation" capabilities of the system.

$$C_s = C(X^{\text{in}}; X^{\text{out}}); \quad C_m = C(X^{\text{in}}; Y^{\text{out}}) \quad (2)$$

$$V_{s,jn} = \langle X^{\text{out}}; X^{\text{out}} \rangle - C(X^{\text{out}}; Y^{\text{out}}) \quad (3)$$

where for two operators A and B we define

$$C(A; B) = \frac{\langle A; B \rangle^2}{\langle A; A \rangle \langle B; B \rangle} \quad \text{with} \quad (4)$$

$$\langle A; B \rangle = \int_{-\infty}^{\infty} e^{i\omega t} \langle A(t) B + B A(t) \rangle dt \quad (5)$$

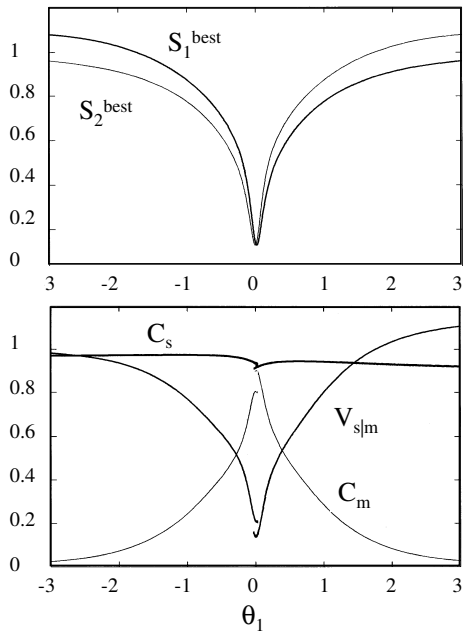


FIG. 4: Top: Best squeezing of the fields for $Y = 1:1$ across the cavity scan. Bottom: QND parameters for $Y = 0:9$, across the cavity scan. Parameters are as in Fig.3 and $\beta = 0$.

The superscripts in and out refer to the input and output fields from the cavity. By calling ϕ_j^{in} and ϕ_j^{out} the phases of the input and output fields in steady state, and choosing field 1 as the meter and field 2 as the signal, we define $X^{\text{out(in)}} = X_2^{\text{out(in)}}$ and $Y^{\text{out}} = Y_1^{\text{out+}} = 2$. For an ideal QND measurement $C_m = C_s = 1$, and $V_{s|j} = 0$. Despite the fact that the two fields have different intracavity intensities at $\theta_1 = 0$, they play here symmetrical roles for the QND scheme; the figure corresponding to the reversed scheme (Fig. 2) being obtained by reflection of the plots $\theta_1 \rightarrow -\theta_1$. If the amplitudes of the two injected fields are not equal (e.g. $|\alpha_2| \neq |\alpha_1|$) the switching of the stable solutions between the high and the low intensity curves disappears (I_1 is always on the low intensity curve). The QND measure is still effective in this case but the symmetry in the role of the two fields is lost: field 2 should be the signal and field 1 the meter. We show in Fig. 5 the frequency dependence of the quantum correlations both above and below Y_{TP} for $\beta = 10$. Although we concentrate here on the good cavity limit which we can analyze with a simple analytical model, squeezing and QND correlations between the two modes persist also in the bad cavity limit. For example for $\beta = 0.5, C = 50, \beta = 3$, equal input intensities 10% below Y_{TP} , $\theta_1 = 0.01$, and for $\beta = 0.1$ we get: $C_s = C_m = 0.72, V_{s|j} = 0.26$.

We wish now to interpret the numerical results with a simple analytical model. The analytical solution of semiclassical equations of the system at steady state is given in [11]. By expanding the steady state polarizations

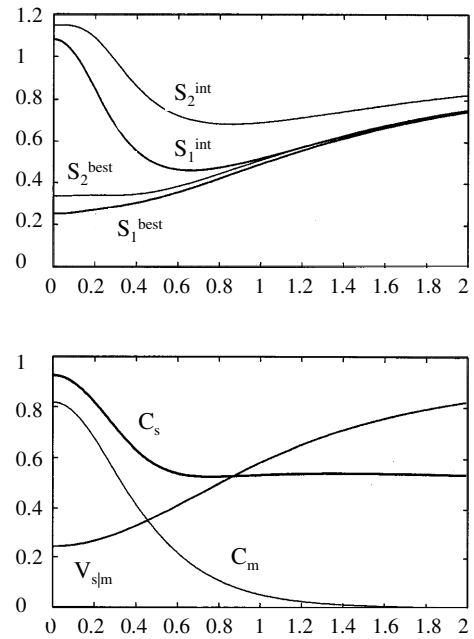


FIG. 5: Top: Best and amplitude quadrature squeezing spectra of the two fields S_j^{best} and S_j^{int} for $Y = 1:1$. Bottom: Frequency dependence of the QND coefficients for $Y = 0:9$. $\theta_1 = 0:09, \beta = 10$ and the other parameters are as in Fig.3.

v and w between levels 1-2 and 3-2 to the first order in β we obtain

$$v = i \frac{4 \alpha_1 \alpha_2 \beta}{(\alpha_1 \beta + \alpha_2 \beta)^2} \quad w = i \frac{4 \alpha_2 \alpha_1 \beta}{(\alpha_1 \beta + \alpha_2 \beta)^2} : \quad (6)$$

By inserting (6) in the semiclassical equations for the intracavity fields amplitudes, with $\dot{\alpha}_j = \alpha_j$ and $C_j = C$, we obtain at steady state a "universal solution" for rescaled field intensities. For $Y < 1$ there are two stable solutions for I_1 and I_2

$$I_1 = \frac{Y}{2} (1 + \sqrt{1 - Y^2}); \quad I_2 = \frac{Y}{2} (1 - \sqrt{1 - Y^2}) \quad (7)$$

$$I_1 = \frac{Y}{2} (1 - \sqrt{1 - Y^2}); \quad I_2 = \frac{Y}{2} (1 + \sqrt{1 - Y^2}) \quad (8)$$

where $\sqrt{1 - Y^2} = \sqrt{1 - Y^2}$. For $Y > 1$, out of the two solutions

$$I_1 = I_2 = I; \quad I = \frac{Y}{2} \left(1 + \frac{1}{Y^2} \right) \quad (9)$$

the one with the plus sign is stable and the other one unstable. Solutions (7)-(9) are indistinguishable from those of the full three-level model in Fig. 2. The phases of the input fields with respect to intracavity fields (which are taken real at steady state) are

$$\phi_1^{\text{in}} = \text{atan} \frac{I_2}{I_1} \quad \phi_2^{\text{in}} = \text{atan} \frac{I_1}{I_2} \quad (10)$$

for $Y < 1$ and

$$\alpha_1^{\text{in}} = \arctan \frac{1}{2I} \quad \alpha_2^{\text{in}} = \arctan \frac{1}{2I} \quad (11)$$

for $Y > 1$. For the output fields $\alpha_1^{\text{out}} = \alpha_1^{\text{in}}$, $\alpha_2^{\text{out}} = \alpha_2^{\text{in}}$ in both cases. In order to study the quantum properties of the system we consider the limit in which the atomic fluctuations follow adiabatically the field fluctuations. In this limit we can construct a simple dynamical model for field fluctuations using the steady state polarizations (6). In this simple model we neglect the noise from spontaneous emission which is however small close to EIT conditions. For $Y > 1$ and $I_1 = I_2 = I$ and taking τ as the unit of time, we obtain

$$\dot{x}_j = -x_j + i \frac{(1)^3}{2I} x_j \quad j = 1; 2: \quad (12)$$

These equations describe two independent two-photon processes for which instabilities and squeezing have been studied extensively [13]. The best squeezing spectrum for each field is

$$S_j^{\text{best}}(\omega) = 1 - \frac{4a}{(1+a)^2 + \omega^2}; \quad a = \frac{1}{2I}; \quad (13)$$

yielding perfect squeezing at zero frequency at the "bistability" turning point where $Y = 1$, $I = 0.5$ and $a = 1$. For $Y < 1$ and $I_1 \neq I_2$ The fluctuations of the two fields are coupled. For $I_1 > I_2$ we get

$$\dot{X}_1 = -X_1 + i \frac{1}{Y} Y_1 \quad (14)$$

$$\dot{Y}_1 = -Y_1 + i \frac{1+}{Y} X_1 - 2j X_2 \quad (15)$$

$$\dot{X}_2 = -X_2 + i \frac{1+}{Y} Y_2 \quad (16)$$

$$\dot{Y}_2 = -Y_2 + i \frac{1}{Y} X_2 - 2j X_1 \quad (17)$$

Simple analytical expressions can be obtained for the squeezing and the conditional variance of the fields at $\omega = 0$

$$S_j^{\text{int}} = S_j^{\text{best}} = 1; \quad S_j^{\text{phase}} = 3 + \frac{4}{2} \quad (18)$$

$$V_{s_{jn}} = \frac{2}{4 - 3^2} \quad (19)$$

showing that the fields have diverging phase noise and become perfectly correlated at the turning point. We show the predictions of the simple model in Fig. 6. In the left panels the input fields intensity Y is varied from 0 to 1, while in the right panels Y is varied from 1 to 1 (on the x-axis of the right figures we have plotted $2 - \frac{1}{Y}$ instead of Y) showing nicely the symmetry in the system between self correlations above and crossed correlations below the bistability threshold. By increasing (from zero)

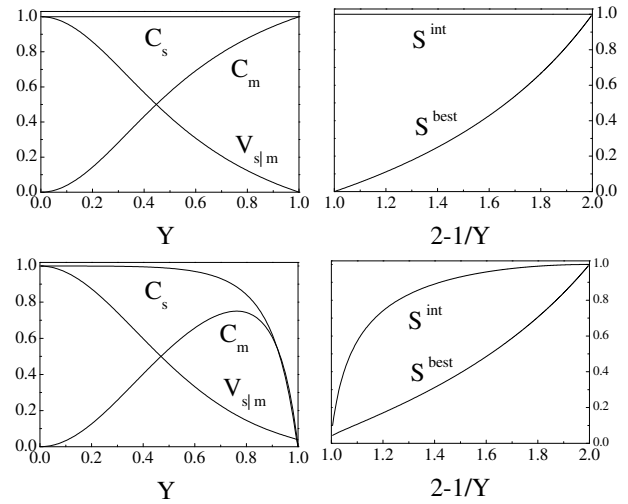


FIG. 6: Quantum correlations for $\alpha_2 = \alpha_1 = 0$ from the simple model as a function of the input fields intensity Y . Top: $I_1 = 0$, bottom: $I_1 = 0.4$.

the analysis frequency, amplitude squeezing appears close to Y_{TP} for $Y > 1$ while for $Y < 1$ the optimum working point for the QND measurement shifts towards smaller values of Y .

I thank L. Lugiato and P. Grangier for useful discussions. Laboratoire Kastler Brossel is UMR 8552 du CNRS de l'ENS et de l'UPMC.

-
- [1] L.V. Hau, S.E. Harris, Z. Dutton, C.H. Behroozi, Nature 397, 594 (1999); D.F. Phillips, A. Fleischhauer, A. Mair, and R.L. Walsworth, M.D. Lukin Physical Review Letters 86, 783 (2001).
 - [2] F. Bardou, J.P. Bouchaud, O. Emile, A. Aspect, and C. Cohen-Tannoudji, Phys. Rev. Lett. 72, 203-206 (1994).
 - [3] O.A. Kocharevskaya, F. M. Auri, E. Arimondo Opt. Comm. 84, 393 (1991).
 - [4] M. Fleischhauer, A. Imamoglu, J.P. Marangos Rev. Mod. Phys. 77, 633 (2005).
 - [5] A. Dantan, M. P. Inard, P.R. Berman, Eur. Phys. Jour. D 27, 193 (2003).
 - [6] D.F. Walls, P. Zoller Opt. Comm. 34, 260 (1980); D.F. Walls, P. Zoller, M.L. Steyn-Ross IEEE Journ. of Quant. Electr. 17, 380 (1981).
 - [7] K.M. Gheri, D.F. Walls, M.A. Marte, Phys. Rev. A 50, 1871 (1994).
 - [8] C.L. Garrido Alzar, L.S. Cruz, J.G. A. Guirre Gomez, Euphys. Lett. 61, 485 (2003).
 - [9] V.A. Sautenkov, Y.V. Rostovstev, M.O. Scully, Phys. Rev. A 72, 065801 (2005).
 - [10] P. Grangier, A. Levenson, J.-P. Poizat, Nature 396, 537 (1998).
 - [11] A. Sinatra, J.-F. Roch, K. Vigneron, P. Grangier, J.-P. Poizat, K. Wang, P. Grangier, Phys. Rev. A 57, 2980 (1998).
 - [12] J.-F. Roch, K. Vigneron, P. Grangier, A. Sinatra, J.-P. Poizat, P. Grangier, Phys. Rev. Lett. 78, 634 (1997).

[13] L. Lugiato, P. Galatola, L. Narducci, *Opt. Comm.* **76**,
276 (1990).